Available online at www.sciencedirect.com

ScienceDirect

Organic Electronics 8 (2007) 683–689

Organic Electronics

www.elsevier.com/locate/orgel

Four-wavelength white organic light-emitting diodes using 4,4′-bis-[carbazoyl-(9)]-stilbene as a deep blue emissive layer

C.H. Jeong *, J.T. Lim, M.S. Kim, J.H. Lee, J.W. Bae, G.Y. Yeom

Department of Advanced Materials Science and Engineering, SungKyunKwan University, Suwon, Gyonggi-Do 440-746, Republic of Korea

Received 13 June 2006; received in revised form 5 March 2007; accepted 17 May 2007
Available online 26 May 2007

Abstract

White organic light-emitting diodes (WOLEDs) with four wavelengths were fabricated by using three doped layers, which were obtained by separating recombination zones into three emitter layers. Among these emitters, blue emissions with two wavelengths (456 and 487 nm) were occurred in the 4,4′-bis(carbazoyl-(9))-stilbene (BCS) host doped with a perylene dye. Also, a green emission was originated from the tris(8-quinolinolato)aluminum (III) (Alq_3) host doped with a green fluorescent of 10-(2-benzothiazolyl)-1,1,7,7-tetramethyl-2,3,6,7-tetrahydro-1H,5H,11H-[1]benzopyrano [6,7,8-*ij*]-quinolizin-11-one (C545T) dye. Finally, an orange emission was obtained from the *N*,*N*′-bis(1-naphthyl)-*N*,*N*′-diphenyl-1,1′-biphenyl-4,4′-diamine (NPB) host doped with a 4-(dicyanomethylene)-2-*tert*-butyl-6-(1,1,7,7-tetramethyljulolidyl-9-enyl)-4H-pyran (DCJTB) dye. The white light could be emitted by simultaneously controlling the emitter thickness and concentration of fluorescent dyes in each emissive layer, resulting in partial excitations among those three emitter layers. Electroluminescent spectra of the device obtained in this study were not sensitive to driving voltage of the device. Also, the maximum luminance for the white OLED with the CIE coordinate of (0.34, 0.34) was 56,300 cd/m^2 at the applied bias voltage of 11.6 V. Also, its external quantum and the power efficiency at about 100 cd/m^2 were 1.68% and 2.41 lm/W, respectively.

PACS: 79.60.Fr; 78.55.Kz; 85.60.Pg

Keywords: WOLED; White emission; BCS; Energy transfer; Carrier trapping; Doping

1. Introduction

In the last few years, white light emission of organic light-emitting diodes (OLEDs) has become increasingly popular as one of the major methods to fabricate full-color display combined with red-green-blue (RGB) color filters, as a flat panel display backlight, and as general solid-state lighting applications [1].

In order to obtain white light emission from the OLEDs, the simultaneously excitation of more than one molecular species in different emissive layers is required because the luminescence of a single organic molecule does not span the entire visible spectrum. White-light emission can be obtained by mixing two complementary colors (e.g., red/bluish-green,

---

* Corresponding author. Tel.: +82 31 299 6562; fax: +82 31 299 6565.

E-mail address: hyuny517@skku.edu (C.H. Jeong).

1566-1199/$ - see front matter © 2007 Elsevier B.V. All rights reserved.
doi:10.1016/j.orgel.2007.05.005

blue/orange, or green/magenta) or three primary colors (red, green, and blue) from small-molecules and/or polymers [1–10].

White light emission is mainly achieved by modifying the spectral characteristics of OLEDs. First, a doping method [2] using a luminescent dye can be used to occur energy transfer from the host to the dopant, or to take place carrier trapping directly at a dopant site [3]. Thus, by using two or three layers doped with different dyes, white light emission can be obtained [1,3–7]. Second, the spatial tuning of the exciton recombination zone can be used by a carrier-blocking layer that preferentially blocks one type of carrier between the hole-transporting layer (HTL) and electron-transporting layer (ETL). Controlling the thickness of this blocking layer enables exciton formation in both the HTL and ETL. If the layers themselves are emissive or contain lumophore dopants, simultaneous emission from the two layers can be achieved, leading to the appropriate color balance. Third, white light emission can be induced by confining each exciton of RGB into different wells of organic multiple quantum-well structures (MQWs), in which the injected carrier distributes in different light-emitting wells [8]. And last, the formation of either excimers (among homolayers) or exciplexs (among heterolayers) can lead to the white emission [1]. These are due to the complicated intermolecular interactions between donor and acceptor consisted of two blue-emitting organic molecules of different electron affinities. Among the above technologies for white emission, first two methods have been used most widely in obtaining white light emission.

For the application of white OLEDs (WOLEDs), the following four issues need to be resolved. One is the shift of color with the increase of the applied bias voltage, due to the movement of carrier recombination zone over the light emitting layers. Second is the mismatch of a luminance and luminous efficiency among the sub pixels of RGB colors as a function of the life time. Third is the achievement of a stable green light among RGB colors by preventing cascade energy transfer between the emissive multilayers [9]. The last is the improvement of the luminous efficiencies further for commercialization. Therefore, the unchangeable color coordinates and the stable exciton recombination with respect to the applied bias voltage in the emitting layers are essential in the successful performance of WOLEDs.

In this study, to obtain highly efficient and highly stable WOLEDs, the OLEDs generating four-wavelength lights (deep blue, bluish-green, deep green, and orange color) were fabricated and their device characteristics were investigated. Especially, to introduce strong blue emission at 450 nm to WOLED, 4,4′-bis(carbazoyl-(9))-stilbene (BCS) doped with perylene system was used [11]. Also, to emit deep green emission at 520 nm more effectively and to obtain a device with less color shift with increasing applied voltage, a novel WOLED device structure composed of three layered hetero-structure multilayer preventing cascade energy transfer [1,6–10] was developed. In these devices, high emission efficiencies could be obtained by controlling either the thickness or the doping concentration of the multiple-doped layers.

2. Experimental

Fig. 1 exhibits molecular structures of the organic materials of the WOLEDs investigated in this study. Among the organic materials, BCS which emits blue light was synthesized by using a two-step route containing processes such as a nucleophilic displacement reaction and a conventional McMurry coupling reaction [12].

Fig. 2a shows the schematic configuration of the WOLEDs used in this study. The multilayered WOLED with three different emissive layers was composed of glass/tin-doped indium oxide (ITO, 120 nm)/2-TNATA (35 nm)/NPB (10 nm)/NPB

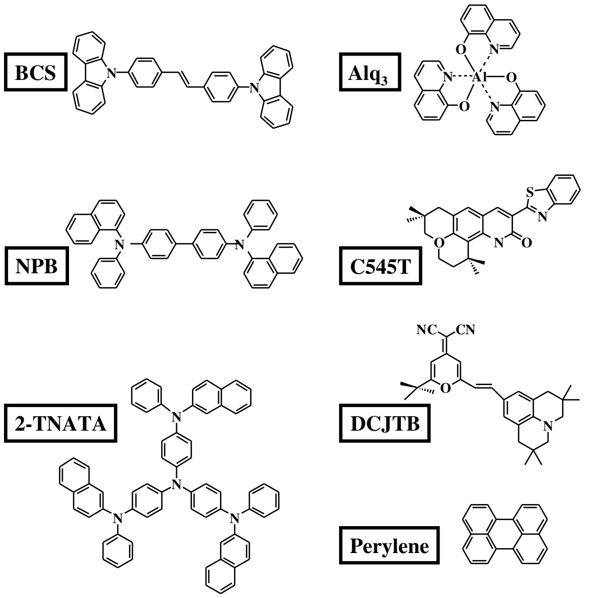

Fig. 1. Molecular structures of the organic materials used in this study.

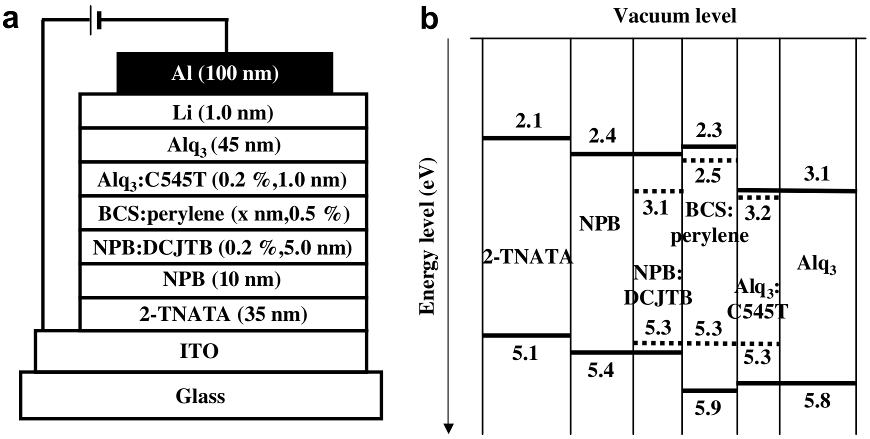

Fig. 2. (a) Schematic diagram of the device structure and (b) energy levels of the organic materials used in this study.

(5.0 nm):DCJTB (0.2 wt%)/BCS (x nm, $x = 10$, 8, and 6, respectively):perylene (0.5 wt%)/Alq$_3$ (1.0 nm):C545T (0.2 wt%)/Alq$_3$ (45 nm)/Li (1.0 nm)/Al (100 nm). ITO (anode) coated on the glass (0.7 mm) has the sheet resistance of about 10 Ω/□. Here, Alq$_3$ is tris(8-quinolinolato) aluminum (III), C545T is 10-(2-benzothiazolyl)-1,1,7,7-tetramethyl-2,3,6,7-tetrahydro-1H,5H,11H- [1] benzopyrano [6, 7,8-*ij*]-quinolizin-11-one, NPB is *N*,*N*′-bis(1-naphthyl)-*N*,*N*′-diphenyl-1,1′-biphenyl-4, 4′-diamine, and DCJTB is 4-(dicyanomethylene)-2-*tert*-butyl-6-(1,1, 7,7-tetramethyljulolidyl-9-enyl)-4H-pyran.

In the WOLEDs, the 4,4′,4″-tris(2-naphthylphenyl-1-phenylamino)triphenylamine (2-TNATA) and NPB layers are used as the hole-injecting layer (HIL) and HTL, respectively. Three emitter layers were used to emit different colors by doping a dopant into the host. The NPB layer doped with the DCJTB dye was used to emit orange color. The BCS layer doped with the perylene dye acted as both the deep blue and bluish-green emitter. The Alq$_3$ layer doped with the C545T was used as the deep green emitter. Alq$_3$, lithium (Li), and aluminum (Al) were used as the ETL, as the electron-injecting layer (EIL), and as the cathode, respectively.

Before loading ITO coated on the glass into a deposition chamber, ITO coated on the glass was cleaned with detergents and deionized water, and dried in the oven at the temperature of 120 °C for 2 h. Devices were fabricated by evaporating both organic materials and metal at the rate of 0.05–0.2 nm/s onto the ITO coated on glass substrate, sequentially at the pressure below 1×10^{-6} Torr. Doping in each emitting layer was simultaneously carried out by co-evaporating both the host and dopant. The emissive active area of the devices was 2×2 mm^2.

Current–voltage–luminance characteristics were measured using a source-measure unit (2400, Keithley Instrument). The intensities from the emission of WOLEDs devices were measured by the photocurrent induced on the silicon photodiodes using a picoammeter (485, Keithley Instrument). The photoluminescence excitation (PLE) and photoluminescence emission (PL) spectra of the deposited OLED materials were measured using luminescence spectrometer (AMINCO Bowman series2, Thermo Spectronic). The electroluminescent (EL) spectra of the as-fabricated devices were measured by optical emission spectroscopy (PCM-420, SC Technology).

3. Results and discussion

As shown in Fig. 2a, WOLEDs investigated in this study are composed of glass/ITO (120 nm)/2-TNATA (35 nm)/NPB (10 nm)/NPB (5.0 nm): DCJTB (0.2 wt%)/BCS (x nm):perylene (0.5 wt%)/ Alq$_3$ (1.0 nm):C545T (0.2 wt%)/Alq$_3$ (45 nm)/Li (1.0 nm)/Al (100 nm).

The light emission from the dopant molecules in all emissive layers are known to be occurred by either energy transfer or carrier trapping [13]. In general, a significant spectral overlap, i.e. overlap of the host emission and the dopant absorption is a key requirement for the efficient energy transfer, whereas for the efficient hole or electron trapping, the HOMO/LUMO energy levels of the dopant must fall within the energy gap of the host. Fig. 2b shows the energy levels (the ionization potential (IP) and the electron affinity (EA)) of 2-TNATA as HIL, NPB as HTL, NPB doped with DCJTB as the orange-emitting layer, BCS doped with perylene as the blue-emitting emitter, Alq_3 doped with C545T as the green-emitting emitter, and Alq_3 as ETL, respectively. As shown in the energy levels of the three emissive layers of Fig. 2b, the HOMO/LUMO of all fluorescent dopant exists within those of the corresponding host. Specially, among the three emissive layers, the BCS doped with perylene is expected to have some hole trapping effect. This is because the IP energy level (5.3 eV) of perylene is located well within the energy gap of the BCS, therefore, it can function as a deep trap in the perylene doped BCS layer. In addition, an electron injection from the C545T doped Alq_3 layer would be expected to be efficiently injected to a dopant rather than the host. This is attributed to the electron injection barrier between Alq_3 (EA: 3.1 eV) and BCS (EA: 2.3 eV) is higher than that between Alq_3 and perylene (EA: 2.5 eV). However, it does not mean that there will be no emission by the energy transfer effect (Foster energy transfer) which is enhanced by the overlapping between the absorption spectrum of the perylene as an acceptor and the emission spectrum of the BCS host as a donor [14]. Therefore, PLE and PL spectra of BCS thin film as well as the PL spectra of BCS doped with perylene were investigated.

Fig. 3 shows the PLE and PL spectra of BCS thin film as well as the PL spectra of BCS doped with perylene (0.5%). As shown in the figure, PLE and PL spectral peaks of BCS were located at 360 and 430 nm, respectively. Also, BCS doped with perylene showed the PL spectrum with two peaks located at 456 and 487 nm, showing the emission characteristic by perylene rather than BCS. Mi et al. [15] reported that the PL spectrum of perylene has two peaks at 446 and 472 nm and its absorption spectrum at 412 and 436 nm. Therefore, it can be seen that the PL spectrum of BCS is largely overlapped with the absorption peak of perylene, which is the condition of EL by Foster energy transfer. Therefore, not only the hole trapping but also Foster energy transfer play an important role in the EL spectrum from the perylene doped BCS layer even though it is difficult to tell currently which is more responsible for the EL spectra observed.

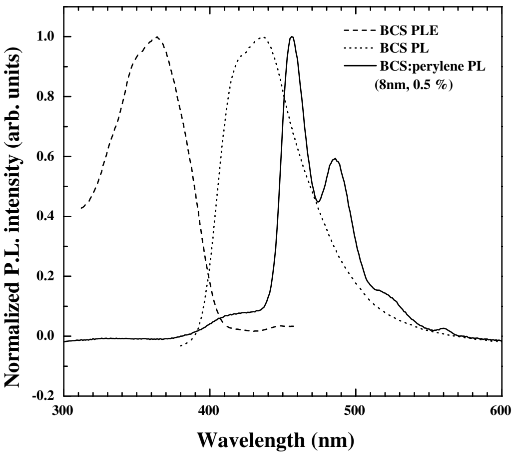

Fig. 3. PLE and PL spectra of BCS thin film and BCS doped with perylene (0.5%) thin film (dash line: BCS PLE, dot line: BCS PL, and solid line: BCS doped with perylene PL, respectively).

In the OLEDs, the luminous efficiency and life time of an emissive layer can be generally improved by doping a dopant into the host layer. Also the emission spectra of the DCM-series (for example: DCJTB, DCM2 [16], etc.) doped layers are generally red-shifted from yellow to deep red with increasing the dopant concentration in an organic solid due to the solid-state solvation effect (SSSE) [14]. However, in the case of doping DCM2 to Alq_3, the external quantum efficiency (η_{ext}) and power efficiency (η_{PE}) are decreased with increasing dopant concentration or increasing a doped-layer thickness when the doping concentration and the thickness of a doped layer are higher than 0.5 wt% and 10 nm, respectively, due to the concentration quenching and hole trapping processes. As a result, the current will be decreased by the reduction of a hole mobility in this layer [17]. For the perylene and C545T doped system, when the dopant concentration is higher than 1 wt%, due to the planar structure of the dopant molecules, the aggregation between molecules is increased. Therefore, EL studies show that, if the dopant concentration is higher the 1 wt%, a shoulder at the long-wavelength edge of emission spectrum begins to grow resulting in undesirable hue shift or lowering its luminance efficiency due to concentration quenching [15,18,19]. Therefore, in this study, to improve a luminous efficiency of the WOLEDs, the emissive layers with low dopant concentration were used. Dopant concentrations of DCJTB as an orange, perylene as a blue, C545T as a green dye in each host layer were 0.2, 0.5, and 0.2 wt%, respectively. Also, as shown in the device configuration of Fig. 2a, the thickness for all emissive layers was optimized within the thickness of 10 nm.

In order to tune to the balanced white emission, EL characteristics at the luminance of 100 cd/m^2 was measured as a function of the thickness of BCS doped with perylene between 6 and 10 nm and the results are shown in Fig. 4a. Table 1 also shows photometric properties and a thickness of BCS doped with perylene of 0.5 wt%. Here, for Device 1, Device 2, and Device 3 shown in Table 1, the thicknesses of the BCS doped with perylene layer were 10, 8, and 6 nm, respectively. Among those three devices, the balanced white emission was obtained through Device 2. The EL spectrum of Device 2 was composed of two blue peaks of 456 and 487 nm, one green peak of 518 nm, and one orange peak of 560 nm. And these peaks were originated from the three emissive layers doped with low concentration dopants. Two blue peaks of 456 and 487 nm composing of the EL spectra are generated by the dopant excitation through both by Foster energy transfer and by carrier trapping at the dopant site (as mentioned in Figs. 2 and 3) because the EL spectrum of the OLED having BCS as the emissive layer should have the maximum peak at the wavelength of 425 nm [11]. Also, similar to the EL result of the perylene-doped OLED investigated by other researchers, two blue peaks instead of one blue peak could be obtained [15]. The green peak at 518 nm is estimated to be occurred by carrier trapping at the C545T molecule site or by the energy transfer from Alq$_3$ to C545T [18–20]. Meanwhile, the orange peak at 560 nm is estimated to be generated by either partial energy transfer from NPB to DCJTB (about 550 nm) due to the incompletely overlaps between the emission spectrum of NPB and the absorption spectrum of DCJTB, or the carrier trapping effect at the DCJTB site [6,16].

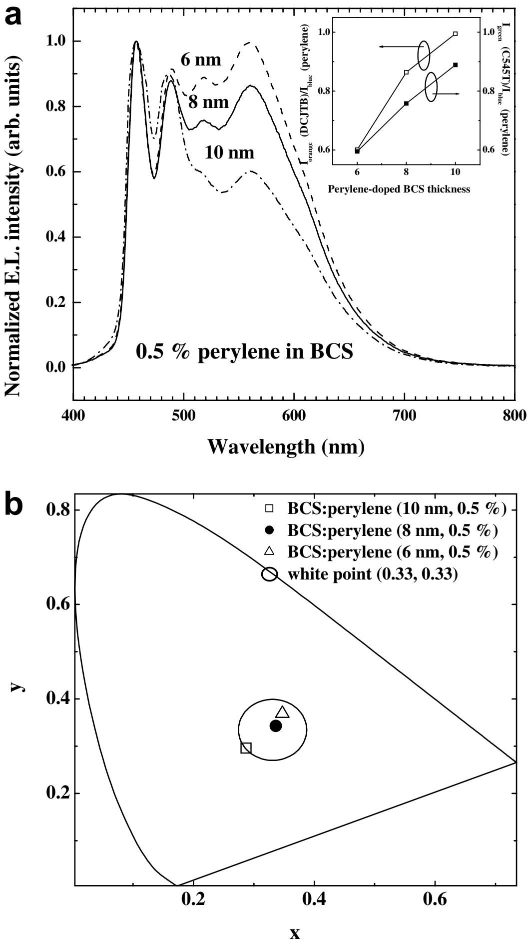

Fig. 4. (a) Effect of the BCS deped with perylene thickness on the normalized EL spectra of the devices composed of glass/ITO (120 nm)/2-TNATA (35 nm)/NPB (10 nm)/NPB (5.0 nm): DCJTB (0.2 wt%)/BCS (x nm):perylene (0.5 wt%)/Alq$_3$ (1.0 nm): C545T (0.2%)/Alq$_3$ (45 nm)/Li (1.0 nm)/Al (100 nm) ($x = 10$ (dash dot line), 8 (solid line), 6 (dash line), respectively), at the applied bias voltage of about 7 V (corresponding to the luminance of 100 cd/m^2). Inset: variation of the EL intensity ratios of I_{orange}(DCJTB)/I_{blue}(perylene) (open square) and I_{green} (C545T)/I_{blue}(perylene) (closed square) as a function of BCS doped with perylene thickness. (b) The CIE chromaticity diagram for the same devices.

The inset of Fig. 4a shows the variation of the EL intensity ratios of I_{orange} (DCJTB)/I_{blue} (perylene) and I_{green} (C545T)/I_{blue} (perylene) as a function in the BCS doped with perylene thickness. As shown in the figure, the decrease of the perylene doped BCS layer thickness from 10 to 6 nm increased the intensity ratios of I_{orange} (DCJTB)/I_{blue} (perylene) and I_{green} (C545T)/I_{blue} (perylene). In fact, more exciton recombination was occurred in the DCJTB and C545T as the BCS doped with perylene thickness was decreased. This is attributed to energy levels of the BCS material having a high electron-blocking property from the Alq$_3$ doped with C545T layer to NPB doped with DCJTB layer and a hole blocking property from the NPB doped with DCJTB layer to Alq$_3$ doped with C545T layer as shown in the energy level in Fig. 2b. Therefore, as the perylene doped BCS layer thickness was decreased, the green- and orange-emission intensities were increased compared to the blue one. In addition, as the thickness of perylene doped BCS layer was decreased, the wavelength range of the white EL spectra was slightly broaden. Fig. 4b shows the corresponding Commission Internationale d'Eclairage (CIE) chromaticity coordinates for the EL spectra of Devices 1–3. The CIE chromacity

Table 1
Turn-on voltage (V_T), current density (J), power efficiency (η_{PL}), external quantum efficiency (η_{ext}), CIE coordinate, and maximum luminance (L_{max}) of WOLEDs for various thickness (t) of BCS doped with perylene

	Device 1	Device 2	Device 3
Thickness of the perylenedoped BCS layer (x nm, 5 wt%)	10	8	6
V_T[a]	3.2	3.2	3.2
J (mA/cm^2)[b]	2.38	2.25	2.17
η_{PL} (lm/W)[b]	2.00	2.41	2.61
η_{ext} (%)[b]	1.42	1.68	1.72
CIE coordinates[b]	(0.29, 0.30)	(0.34, 0.34)	(0.35, 0.37)
L_{max} (cs/m^2)	55,200 at 11.8 V	56,300 at 11.6 V	55,300 at 11.4 V

[a] The turn-on voltage was measured at the luminance of 0.1 cd/m^2.
[b] The data were measured at 100 cd/m^2.

coordinates for Devices 1–3 at the luminance of 100 cd/m^2 were (0.29, 0.30), (0.34, 0.34), and (0.35, 0.37), respectively. Therefore, Device 2 is the closest to white point of (0.33, 0.33) among the WOLEDs investigated.

Fig. 5 shows white EL spectra as a function of the applied bias voltage for Device 2 having 8 nm-thick BCS doped with perylene (0.5 wt%) and the inset of Fig. 5 exhibits the CIE coordinates for corresponding EL spectra. As shown in the inset of Fig. 5, as the voltage increased from 4 (the corresponding luminance of 1.40 cd/m^2) to 9 V (1610 cd/m^2), the corresponding CIE chromaticity coordinates of EL spectra showed nearly unchangeable characteristic within the range of (0.34–0.35, 0.34–0.35). This stability of the coordinates obtained in our devices is attributed to the stable exciton recombination in each emissive layer for the bias voltages investigated.

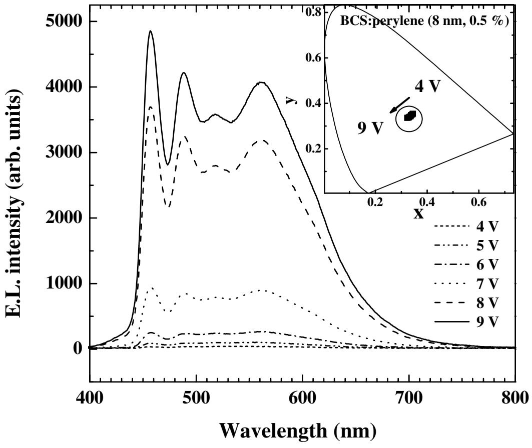

Fig. 5. Spectral variation as a function of the applied bias voltage (4–9 V) for Device 2. The inset shows the corresponding CIE chromaticity coordinates for the same device. The white point is CIE chromaticity coordinates of (0.33, 0.33).

Fig. 6a shows the current density (J) and luminance (L) of the Devices 1–3 as a function of applied bias voltage. The maximum luminance of the devices are also shown in Table 1. As shown in Fig. 6a and Table 1, the maximum luminance (L_{max}) were 55,200 (11.8), 56,300 (11.6), and 55,300 cd/m^2 (11.4 V) for Device 1, Device 2, and Device 3, respectively. And the turn-on voltages at the luminance of 0.1 cd/m^2 for Devices 1–3 were 3.2, 3.2, and 3.2 V, respectively. Also, as the perylene-doped BCS thickness was increased in the OLEDs, the current density at the same applied bias voltage was slightly increased. Especially for the operating voltage was lower than 3 V, when the thickness of the perylene doped BCS was 6 or 8 nm, the $J-V-L$ characteristics were similar each other and showed good properties, however, when the thickness was 10 nm, the current–voltage characteristic was a little degraded. Even though the device operating mechanism needs more investigation, the change of electrical properties appears to be related to the high hole-blocking and high electron-blocking properties of BCS.

Fig. 6b shows the power efficiency (η_{PE}) and external quantum efficiency (η_{ext}) as a function of current density (J) for Devices 1–3. Device 2 having the CIE coordinate close to the white point exhibited η_{PE} of 2.25 lm/W at the luminance of about 100 cd/m^2. The η_{PE} values at about 100 cd/m^2 for Device 1 and Device 3 were 2.00 and 2.61 lm/W, respectively. Also, the values of η_{ext} for Devices 1–3 were 1.42%, 1.68%, and 1.72%, respectively. Therefore, as the thickness of perylene doped BCS layer was decreased, η_{PE} and η_{ext} of the device were increased. Therefore, the luminous efficiencies, that is, both η_{PE} and η_{ext} were the highest for Device 3 among Devices 1–3. The differences of the luminous efficiencies obtained in our devices are also believed

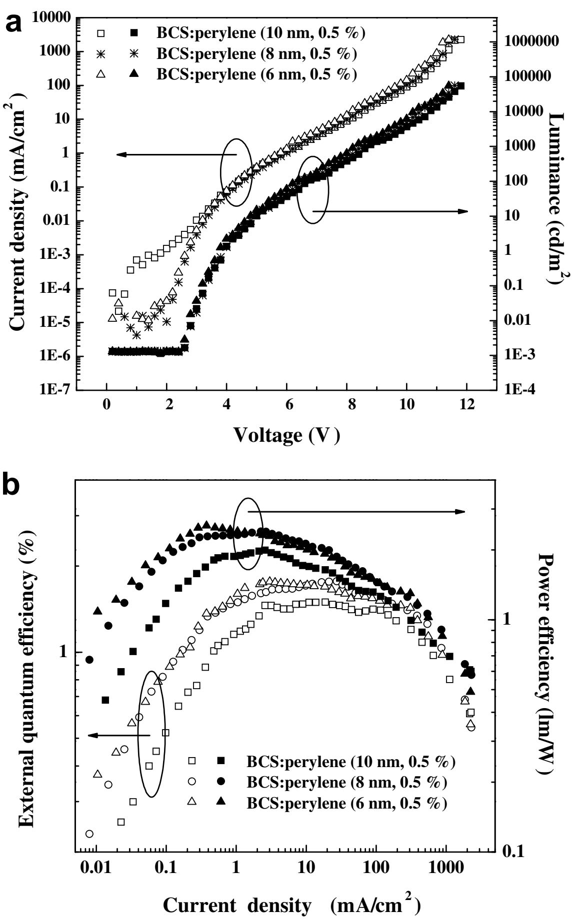

Fig. 6. (a) Current density–voltage–luminance characteristics for Devices 1–3 composed of glass/ITO (120 nm)/2-TNATA (35 nm)/NPB (10 nm)/NPB (5 nm):DCJTB (0.2 wt%)/BCS (x nm):perylene (0.5 wt%)/Alq$_3$(1.0 nm):C545T (0.2 wt%)/Alq$_3$ (45 nm)/Li (1.0 nm)/Al (100 nm) (square: 10, star: 8, and triangle: 6, respectively). (b) External quantum efficiency and power efficiency as a function of current density for the same devices (square: 10, circle: 8, and triangle: 6, respectively).

to be closely related to the carrier-blocking property.

4. Conclusions

Four-wavelength emitting WOLEDs were successfully fabricated by using three doped emissive layers and by separating each recombination zone in the three emitter layers. Also, the very bright and highly efficient WOLEDs with the $L_{\max}$ exceeding 55,000 cd/m^2 and with the η_{PE} of up to 2.62 lm/W could be demonstrated. The white light was originated from the partial excitation of fluorescent dyes composing the doped systems by controlling the layer thickness and concentration of each fluorescent dye in the emissive layers. EL spectra of the white light-emitting device investigated in this study were not highly sensitive to deriving voltages investigated in this study, therefore, the color coordinates of the devices were well within white range with increasing the bias voltage. The WOLED device with the CIE coordinate of (0.34, 0.34) showed the maximum luminance of 56,300 cd/m^2 and at the luminance of about 100 cd/m^2, η_{ext} and η_{PE} of the devices were 1.68% and 2.41 lm/W, respectively.

Acknowledgements

This work was supported by the National Research Laboratory Program (NRL) of the Ministry of Science and Technology and by the Ministry of Commerce, Industry and Energy (MOCIE).

References

[1] B.W. D'Andrade, S.R. Forrest, Adv. Mater. 16 (2004) 1585.
[2] C.W. Tang, S.A. Van Slyke, C.H. Chen, J. Appl. Phys. 65 (1989) 3610.
[3] J. Kido, W. Ikeda, M. Kimura, K. Nagai, Jpn. J. Appl. Phys. 35 (1996) L394.
[4] J. Kido, M. Kimura, K. Nagai, Science 267 (1995) 1332.
[5] R.H. Jordan, A. Dodabalapur, M. Strukelj, T.M. Miller, Appl. Phys. Lett. 68 (1996) 1192.
[6] R.S. Deshpande, V. Bulovic, S.R. Forrest, Appl. Phys. Lett. 75 (1999) 888.
[7] C.W. Ko, Y.T. Tao, Appl. Phys. Lett. 79 (2001) 4234.
[8] Z.Y. Zie, Y.Q. Li, J. Feng, J.S. Huang, Y. Wang, C.N. Li, S.Y. Liu, J.C. Shen, Synth. Metals 106 (1999) 71.
[9] M. Berggren, A. Dodabalapur, R.E. Slusher, Z. Bao, Nature 389 (1997) 466.
[10] J. Liu, Q. Zhou, Y. Cheng, Y. Geng, L. Wang, D. Ma, X. Jing, F. Wang, Adv. Mater. 17 (2005) 2974.
[11] H.S. Woo, S.J. Cho, T.W. Kwon, D.K. Park, J. Korean Phys. Soc. 46 (2005) 981.
[12] T. Mukaiyama, T. Sato, J. Hanna, Chem. Lett. 10 (1973) 1041.
[13] D.M. Roundhill, J.P. Fackler, Optoelectronic Properties of Inorganic Compounds, Plenum Press, 1999.
[14] M. Anni, G. Gigli, V. Paladini, R. Cingolani, G. Barbarella, L. Favaretto, G. Sotgiu, M. Zambianchi, Appl. Phys. Lett. 77 (2000) 2458.
[15] B.X. Mi, Z.Q. Gao, C.S. Lee, S.T. Lee, H.L. Kwong, N.B. Wong, Appl. Phys. Lett. 75 (1999) 4055.
[16] V. Bulovic, A. Shoustikov, M.A. Baldo, E. Bose, V.G. Kozlov, M.E. Thompson, S.R. Forrest, Chem. Phys. Lett. 287 (1998) 455.
[17] K.O. Cheon, J. Shinar, Appl. Phys. Lett. 81 (2002) 1738.
[18] C.H. Chen, C.W. Tang, Appl. Phys. Lett. 79 (2001) 3711.
[19] K. Yamashita, J. Futenma, T. Mori, T. Miutani, Synth. Metals 111–112 (2000) 87.
[20] J. Littman, P. Martic, J. Appl. Phys. 72 (1992) 1957.